Evaluation of Combined Visible/NIR Camera for Iris Authentication on Smartphones

Shejin Thavalengal[1,2], Petronel Bigioi[1,2] and Peter Corcoran[2].
[1]FotoNation Ltd, Galway, Ireland.
[2]National University of Ireland Galway, Galway, Ireland.
{sthavalengal,pbigioi}@fotonation.com, peter.corcoran@nuigalway.ie

Abstract

Iris biometrics provide a mature and robust method of authentication, but are typically applied in a controlled environment and under constrained acquisition conditions. In this paper, the adaption of iris biometrics for unconstrained, hand-held use cases such as smartphones is investigated. A prototype optics-sensor combination is analysed in terms of its optical properties and iris imaging capabilities. The corresponding camera system with dual visible/NIR sensing capabilities and 4 Megapixel resolution is tested for suitability to implement iris recognition on smartphones. Recognition performance is analysed together with image quality comparisons. Preliminary results indicate that there are challenges to achieve reliable recognition performance in unconstrained use cases. Current optical systems are not diffraction limited, particularly at NIR wavelengths; pixel resolutions are close to the useful limits for iris recognition and acquisition conditions are challenging. Nevertheless, our findings indicate a similar camera module, with an improved optics and sensor, could combine biometric authentication with more conventional front-camera functions such as the capture of selfie images.

1. Introduction

Smartphones are omnipresent nowadays and it is expected to have 2 billion people using smartphones in 2016 [10]. This is predicted to grow to a third of the world's population in 2018. Reliable assessment of the smartphone user's identity will be crucial as data such as sensitive personal information, financial transactions and user generated content will be generated and transmitted via these devices. Some researchers have even postulated that smartphones may become mandatory to identify their owner [8]. Face and fingerprint biometrics enabled smartphones are already available.

The iris of the human eye is considered to be a near ideal biometric [5, 11] but is yet to be introduced in smartphones. This is at least in part due to the constrained nature of current iris acquisition devices and the inability of current smartphone cameras to acquire high quality iris images in the NIR spectrum. In contrast, acquisition on hand-held devices introduces a challenging set of conditions : - uncontrolled illumination condition, limited processing power, optical constraints introduced by miniature camera modules, pixel resolution limited by optical and cost considerations, an unstable hand-held platform introducing motion blur artefacts, and an unconstrained moving object - the human eye. Unconstrained iris acquisition systems do exist in airports and other public access use cases, but such systems can employ high-end optical systems, control on lighting, and optical and image sensing subsystems that are not size constrained. These systems are also provided with a stable mount, and where the subjects is in motion will typically feature multiple cameras.

For smartphones, a typical use case is the user authentication using the front-facing camera, while holding the device at a comfortable arm's length. From the perspective of cost, reusing the same sensor and optics to capture both visible (video call, selfie imaging) and NIR (iris) image data favours a single user-facing camera.

This paper investigates on such an RGB-NIR dual purpose camera option and carry out a feasibility study of iris recognition using such a prototype device.

This paper is organised as follows: Section 2 gives a brief overview of related research on iris recognition on smartphones, Section 3 introduces a dual purpose RGB-NIR camera for smartphone iris recognition. The optical analyses of such a device is given in Section 4. Section 5 deals with the data acquisition and iris recognition experiment using the prototype device introduced in Section 3. Summary of the work and conclusions are given in Section 6.

2. Review of related research

Even though iris recognition is a well-researched area, there have been few studies on implementing iris recognition on smartphone. This may be mainly due to the highly constrained nature of iris recognition systems as well as the inability of existing smartphone cameras to produce adequate quality images for reliable iris recognition performance. One early work in this field shows a cold mirror with IR pass filter (750nm) attached on a Samsung SPH-S2300 camera-phone with 2048 × 1536 pixel CCD sensor and 3x optical zoom [14]. Later Cho, Park, and Rhee [13] improved the localization of pupil and iris regions for the same system. The existing Xenon flash was used as an illumination source in this early research. In a follow up work dual IR illuminators were added to a similarly modified camera-phone [24]. This modified camera system has an operating range of 35-40 cm (with the help of optical zoom) and captures dual eye regions. The user has to align his eyes with the specific area indicated on the cold mirror in order to accurately estimate the eye location. Considering a standard iris of size 11mm, approximately 210 pixels across iris will be present in the images acquired using this set up. In this regard the acquisition process of Park *et al.* [24] is constrained, as the eye pair must be well centred in the region delineated by the cold mirror. Also, the authors failed to mention how they dealt with the IR cut-off filter present in front of the CCD sensor.

A recent line of research on iris recognition using smartphones focuses on the use of iris images captured using the existing smartphone cameras [3, 15, 25]. These cameras capture images in visible wavelength, which may not contain sufficient iris information, especially in dark coloured irises [6, 11]. Also, ISO/IEC 19794-6 and NIST Mobile ID best practice recommend iris images to be captured in near infra-red illumination [23, 30]. Corcoran, Bigioi and Thavalengal carried out a feasibility study and design considerations for an iris acquisition system for smartphones [9]. This work mentioned the idea of a single hybrid camera to use as the front facing camera of the mobile phones, which will perform both iris recognition and act as a general-purpose user-facing camera. Even though this system can be cost effective as compared to using a separate iris recognition camera, it poses some challenges such as (i) a movable NIR optical filter might be needed to support iris acquisition mode, (ii) optical design at visible and NIR wavelengths has to be optimized for two different sets of requirements, but using the same CMOS sensor.

3. Dual Purpose RGB-NIR Camera For Smartphone Iris Recognition

Single sensor digital cameras use colour filter array (CFA) to sample different spectral components. In this kind of arrangement, only one colour is sampled at each pixel location. The most commonly used CFA is a Bayer pattern, which is shown in Figure 1(a) [4]. US 8446470 B2 presented a combined RGB and IR imaging sensor. This sensor replaces half of the green pixels with IR pixels in the normal colour filter array [18]. The colour filter array of such a sensor is shown in Figure 1 (b).

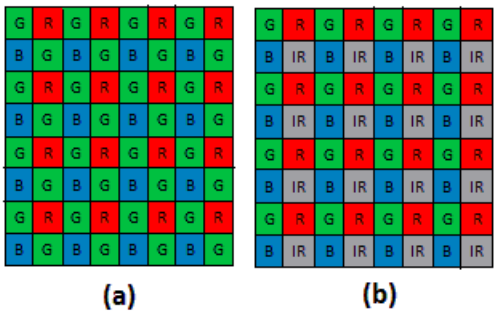

Figure 1. Example for colour filter arrays(CFA) : (a) Bayer CFA, (b) CFA presented in US 8446470 B2. R, G an B represents Red, Green and Blue colour sampling filters respectively. IR represents NIR sampling filter.

This sensor was primarily aimed to use in an imaging system for vehicles to obtain a more accurate true colour representation of the pixels and to limit infra-red colour wash out [18]. Such a sensor could be used in developing a hybrid front facing dual purpose camera for smart phones as explained in [9].

OmniVision's OV4682 is such an RGB-IR single sensor, which is aimed to be used in cellular phones and other digital still cameras [22]. This sensor has a maximum lens chief ray angle of 21degrees, which restricts the focal length of the optical system to be approximately 4mm. We have internally developed a prototype camera of smartphone form factor, which uses such a sensor. The specification of this device is shown in Table 1.

Parameter	Value
Sensor Size	1/3"
Aspect Ratio	16:9
Sensor resolution ($w \times l$)	2688×1520
Pixel size	$2\mu m \times 2\mu m$
Focal length (f)	$4mm$
F number (F)	2
Scan Mode	Progressive
Active Illumination (λ)	$850nm$

Table 1. System Parameters

4. Optical Analysis

This section analyses the suitability of the prototype device for iris recognition. The important camera parameters are shown in Table 1. Considering a typical iris acquisition scenario using smartphones with a stand-off distance $d = 200mm$ and assuming a circle of confusion $c = 2\mu m$, the far point (S) and near point (R) in which the image is in focus are given by [2],

$$[S, R] = \frac{df^2}{f^2 \pm Fcd}, \tag{1}$$

which gives

$$S = 210.53mm, R = 190.48mm. \tag{2}$$

Hence, the Depth of Field (DoF) is,

$$DoF = S - R = 20.05mm. \tag{3}$$

At a stand-off distance of $d = 200mm$, this camera will have a magnification factor M,

$$M = \frac{f}{d - f} = 0.02041. \tag{4}$$

That is, this camera will magnify the iris by 0.02041 on to its sensor. Also, vertical field of view (FoV_v) and horizontal field of view (FoV_h) can be calculated as below [2],

$$FoV_v = 2 \arctan\left(\frac{l}{2f}\right) \tag{5}$$

$$= 2 \arctan\left(\frac{1520 \times 2\mu m}{2 \times 4mm}\right) \approx 42^\circ \tag{6}$$

$$FoV_h = 2 \arctan\left(\frac{w}{2f}\right) \tag{7}$$

$$= 2 \arctan\left(\frac{2688 \times 2\mu m}{2 \times 4mm}\right) \approx 67^\circ. \tag{8}$$

4.1. Equivalent Pixel Dimensions and Optical Resolution

Hence, at $200mm$ stand-off distance, this camera will enable us to capture a horizontal distance,

$$d_h = 2 \tan\left(\frac{FoV_h}{2}\right) \times d \approx 265mm. \tag{9}$$

Similarly, a vertical distance (d_v) of $\approx$ $154mm$ can be obtained. That is, at $200mm$, this camera can provide a capture box of $265mm \times 154mm$ and a depth of field of $20.05mm$. Considering a maximum inter-pupillary distance of $78mm$ [12], this capture box will be sufficient to obtain both eyes simultaneously. Further, assuming an iris of size $11mm$ [11], a magnification of 0.02041 (as shown in 4) will result in an iris image of $224\mu m$ diameter on the sensor. The sensor has a pixel size of $2\mu m$, so assuming a fill factor of 100% the iris will have 112 pixels diameter on the sensor. But, due to the nature of the particular CFA used here, IR values are sampled at alternate locations on the sensor. Hence, the number of true IR pixels across iris will be reduced by a factor of two. That is, in this set up, iris will have 56 true, non-up sampled pixels across the diameter.

Within the depth of field, the iris will have pixel range of 53 to 59 pixels on sensor. This is less than the marginal quality of iris image as outlined in ISO/IEC 19794-6 and NIST Mobile ID best practice [23, 30], but may be acceptable as per the studies shown in [1, 9, 28].

However, valid NIR information would also be available from the RGB pixels (as the colour filters do not block light at 850nm and the global cut off IR filter will have to have a pass band around 850nm to allow the IR pixels to function), which could be used to obtain complimentary information which may help in iris recognition.

4.2. Modulation Transfer Function of Diffraction Limited System

For a perfect optical system, with uniformly illuminated and uniformly transmitting aperture, the modulation transfer function (MTF) can be calculated as [26]

$$MTF_{optics}(\upsilon) = \frac{2}{\pi}(\phi - \cos\phi \sin\phi) \tag{10}$$

where υ is the spacial frequency in $cycles/mm$ and ϕ can be obtained as,

$$\phi = \arccos(F\lambda\upsilon). \tag{11}$$

where F is the F number and λ is active illumination. The limiting resolution for the aberration free system can be calculated as,

$$\upsilon_0 = \frac{1}{F\lambda} = 588.2\ cycles/mm. \tag{12}$$

That is, the optical system presented here cannot transmit information at a higher spatial frequency than $\upsilon_0 = 588.2\ cycles/mm$.

Sensor MTF can be calculated assuming square pixels and 100% fill factor as,

$$MTF_{sensor}(\upsilon) = \text{sinc}\,(\upsilon\delta_x)\,\text{sinc}\left(\upsilon\delta_f\right) \tag{13}$$

where υ is the spacial frequency, δ_x is the pixel pitch, δ_f is the detector footprint and

$$\text{sinc}\,(x) = \frac{\sin(\pi x)}{\pi x}. \tag{14}$$

The system MTF can be calculated as,

$$MTF_{system} = MTF_{optics} \times MTF_{sensor}. \tag{15}$$

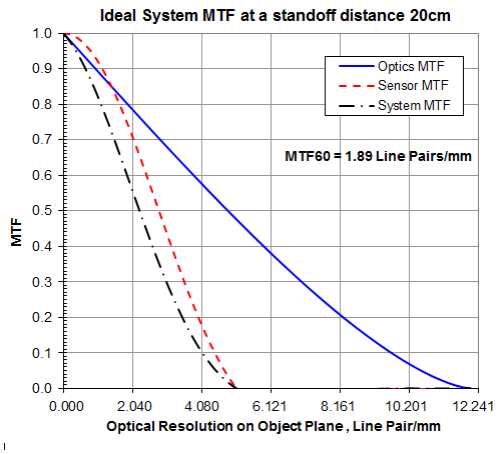

Figure 2. Ideal System Modulation Transfer Function (MTF) plot for 200mm stand-off distance.

The ideal system MTF for the acquisition device presented here is shown in Figure 2. From Figure 2, it can be observed that, at 60% system modulation, this set up provides an optical resolution of 1.89 line pairs/mm (lp/mm) on the object plane. This is less than the 'marginal 'quality of 2 line pairs/mm defined by ISO/IEC 19794-6 standards [30].

Similar analyses can be done on two other stand-off distances - 150*mm* and 250*mm* from the device. The results are summarized in the Table 2.

Parameter	***d=150mm***	***d=200mm***	***d=250mm***
Number of Pixels across iris diameter	72-78	53-59	42-48
Depth of Field	11.21mm	20.05mm	31.37mm
Dual Eye Capture	Yes	Yes	Yes
Optical Resolution at 60% modulation	2.54 lp/mm	1.89 lp/mm	1.51 lp/mm

Table 2. Summary of Optical Analysis for Different Stand-off Distances

From Table 2, it can be observed that images captured at 200*mm* and 250*mm* stand-off distances will be of unacceptable quality as per the ISO standards [30], both in terms of true number of pixels across iris and optical resolution. But, images captured at stand-off distances 200*mm* and 150*mm* will have more than 50 true, non-up sampled pixels across iris diameter, which may contain sufficient information for iris recognition [1, 9]. Images acquired at a stand-off distance 150*mm* is of better quality as compared to the rest two image sets both in terms of number of pixels across iris and optical resolution. The ideal optical resolution at this distance is of 'marginal 'as per ISO standard [30]. Note that, as the stand-off distance decreases, the depth of filed also decreases. Hence a use case where images will be acquired at a distance less than 150*mm* from the smartphone will be highly constrained and user-unfriendly. Also, these properties are calculated assuming ideal optics, 100% fill factor and 100% sensing area for each pixel. The practical system may deviate far from these ideal conditions and hence, can result in reduced image quality.

The practical system modulation transfer function (MTF) at 200*mm* stand-off distance of this device was measured using the Imatest tool [16]. For MTF calculation, NIR images captured with an illumination of 850nm were used. The MTF plot is shown in Figure 3.

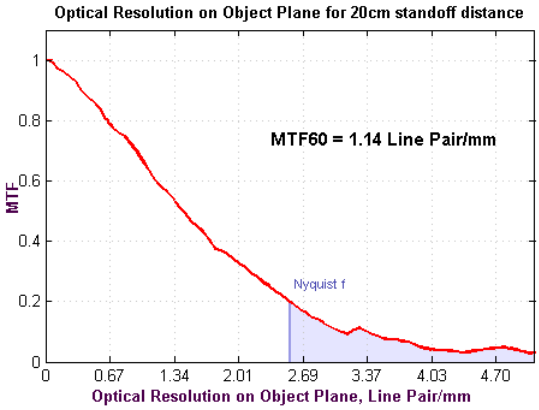

Figure 3. Modulation Transfer Function (MTF) plot for 200mm stand-off distance.

From Figure 3, it can be observed that, at 60% system modulation, this set up provides an optical resolution of 1.14 lp/mm on the object plane. Similarly, for 150*mm* stand-off distance, this will be 1.18 lp/mm. These values are less than the ideal values shown in Table 2 as well as the 'marginal 'quality of 2 lp/mm defined by ISO/IEC 19794-6 standards [30].

4.3. Diffraction Limit Calculation

The radius of the Airy disk, which is a result of the lens diffraction limit, can be calculated for our prototype system ($\lambda = 850nm$, $F = 2$) as,

$$r = 1.22F\lambda, \tag{16}$$

$$= 2.07\mu m. \tag{17}$$

According to Rayleigh criterion, two separate point images can be resolved if the radius of the Airy disk is less than the pixel size. That means, this is the smallest theoretical pixel of detail [2, 20]. In the optical system presented here, the radius of the airy disk is close to the pixel size. However it is clear from the MTF that the lens is far from diffraction-limited.

5. Data Acquisition and Iris Recognition Experiments

The analyses in the previous section (Section 4) show that iris images obtained using our device may not be adequate for iris recognition. In order to experimentally evaluate feasibility of iris recognition on these images, we have gathered a database internally [1]. The database consists of images from 25 subjects acquired at two different distances 15cm and 20cm from the device. Active illumination of 850 nm was used for image capture. Ambient illumination was not constrained while images were acquired. The dataset consist of subject with eye colours varying from blue to dark brown. Iris images are cropped automatically by the face and eye detection algorithms developed internally. The images are then fed to an open source iris recognition algorithm - OSIRIS v4.1 [27]. A total of 244 images were captured at 15cm stand-off distance and 311 images for 20cm stand-off distance.

5.1. Analyses and Observations

Receiver Operating Characteristic (ROC) curves of these experiments is shown in Figure 4. From Figure 4, it can be

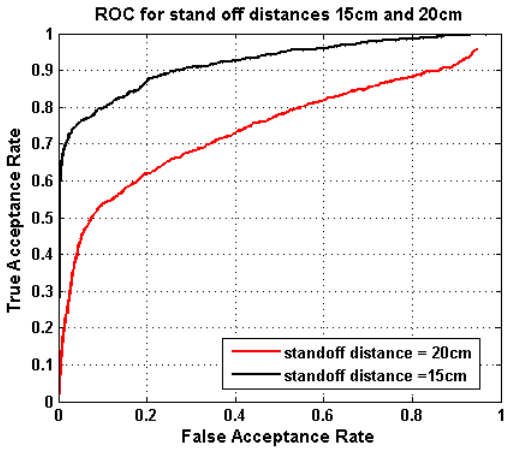

Figure 4. ROC Curves for 15cm and 20cm stand-off distances.

observed that, images captured at a stand-off distance 15cm outperform the images captured at 20cm. This may be due to the fact that the former set of images has a better optical resolution and more number of pixels across iris diameter, and hence more information on the iris region. Further, the score distribution of these two set of experiments are shown in Figure 5, From Figure 5, it can be noted that, inter class comparisons in both cases form a narrow range normal distribution with mean around 0.45 hamming distance. But intra class comparisons shows a wide distribution with considerable overlap with the inter class comparisons.

[1]The database will be made available for research once we have obtained the approval of the research ethics committee of our organization.

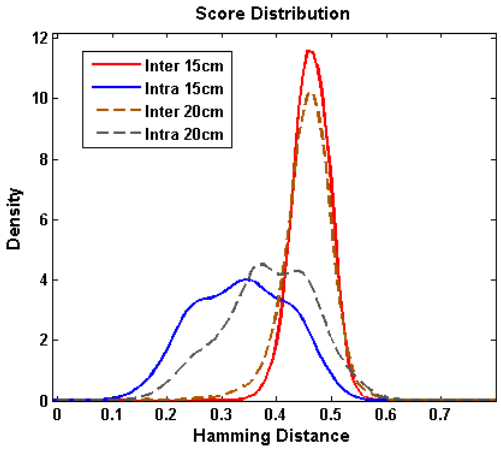

Figure 5. Score distribution for 15cm and 20cm stand-off distances.

A careful analysis revealed that segmentation algorithm failed to detect the iris and pupil accurately on 10.66% and 27.49% images, on 15cm stand-off distance and 20cm stand-off distance cases respectively. This could be a main reason for large hamming distances on intra class comparison. A second set of experiments was carried out after removing the images, in which segmentation algorithm failed to detect an iris or pupil. Images with small segmentation errors were tolerated. The comparison of ROC curves is shown in Figure 6.

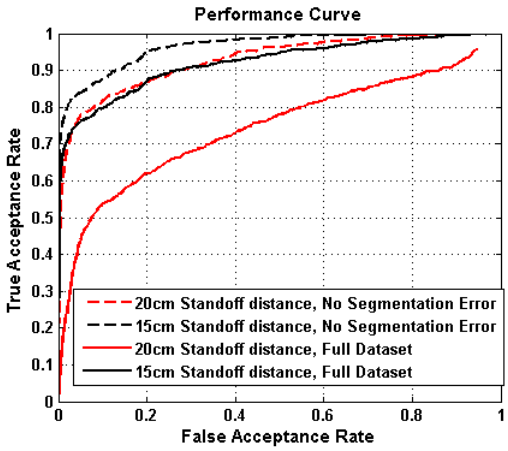

Figure 6. Performance comparison between full image set and image set with improved iris segmentation for 15cm and 20cm stand-off distance.

From Figure 6, it is evident that improving iris segmentation can improve the performance significantly. Score distributions of these experiments were compared with the score distribution of the iris recognition experiments carried out on the full database in Figure 7 and Figure 8.

From Figure 7 and Figure 8, it can be observed that by removing those comparisons in which the iris and pupil

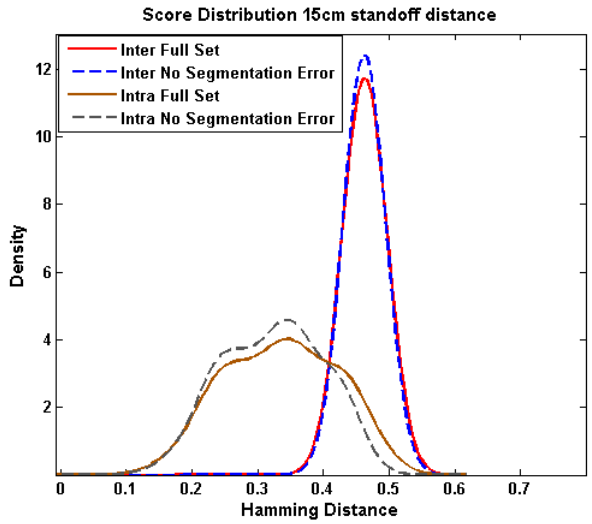

Figure 7. Score distribution comparison for 15cm stand-off distance.

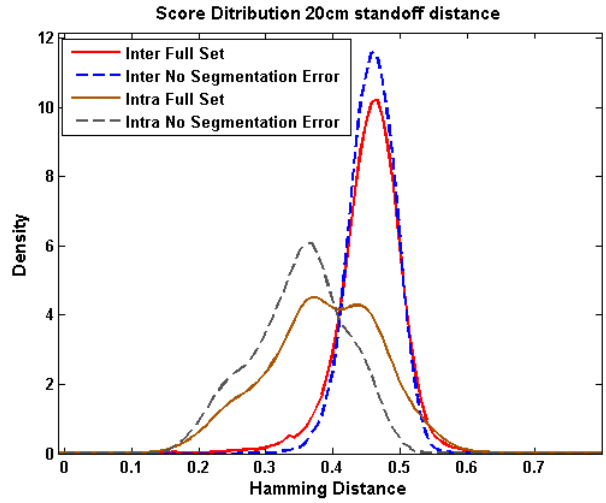

Figure 8. Score distribution comparison for 20cm stand-off distance.

weren't detected accurately, intra class score distribution improved slightly. The remaining large hamming distance cases in the intra class comparisons could be due to the lack of information on the iris region or poor quality images in terms of image sharpness and contrast. One another important observation to be made is that intra class and inter class score distribution of 15cm dataset is less overlapped as compared to that of the 20cm case. This is because of the comparatively better segmentation results on these images and the availability of more iris information due to the better image quality.

This can be analysed by measuring different image quality parameters of the iris images captured using our device and comparing with the images of the existing iris databases. Neurotechnology's VeriEye SDK is used for the image quality analysis [21]. This SDK assign scores for different image parameters such as iris-sclera contrast, iris-pupil contrast, sharpness, usable iris area, pupil to iris ratio, iris pupil concentricity, grayscale utilization, pupil boundary circularity, interlace and margin adequacy. An overall image quality score is also assigned to each image. Larger the score, better the quality of the image [21]. We have measured average iris-pupil contrast, iris-sclera contrast, image sharpness and overall image quality from a representative sample image set on 8 different iris databases. The quality scores are tabulated in Table 3.

Database	Iris to Pupil Contrast Score	Iris to Sclera Contrast Score	Sharpness Score	Overall Image Quality
CASIA V4 Interval [29]	68	11	100	62
CASIA V4 Thousand [29]	95	16	94	40
MMU2 [19]	75	28	100	30
MMU1 [19]	81	22	99	47
IIT Delhi [17]	99	23	100	64
CASIA V4 Distance [29]	58	22	96	34
Our Database (20cm stand-off distance)	38	18	80	28
Our Database (15cm stand-off distance)	43	20	80	30

Table 3. Comparison of iris image quality scores on different databases

From Table 3, it can be observed that, iris images captured using our device have low image quality scores as compared to the other publicly available research databases. The images in these research databases were acquired using a high quality dedicated iris cameras in constrained acquisition scenarios. Also, it can be noted that iris images captured at 15cm have slightly better image quality score as compared to those images captured at 20cm stand-off distance. This is in agreement with the analysis in Section 4.

6. Summary and Conclusions

In this paper we have examined the use of a dual-purpose RGB-NIR front facing camera for smartphones. This camera combines the functionality of a conventional front-camera, such as selfie imaging and video call, with the potential for iris authentication. However there are significant challenges in implementing such a system. Even for a close stand-off distance of 15cm, the optical properties of the system are marginal and pixel resolution for iris recognition is below the minimum threshold defined by the current international standards. Also, due to the novelness of the colour filter array in this visible/NIR sensor, the RGB image quality is likely to suffer when compared to a standard front facing camera with conventional Bayer pattern CFA.

In practice, a high quality image must be acquired in order to successfully segment the iris region. This is particularly important for the challenging hand-held use case presented here. In our experiments more than 27% of acquisitions lead to unsuccessful iris and pupil detection/segmentation at a distance of 20 cm from the camera.

This figure is improved to just over 10% at 15 cm. Also the recognition performance is noted to be lower than the current state of the art, primarily due to the reduced quality of the acquired iris images. Removing such non-segmenting images demonstrates a much more acceptable level of performance. These illustrate the challenge of implementing iris authentication in this unconstrained use case and suggests that the detection of non-segmenting iris regions could help with improving overall performance significantly.

However the best improvement would be achieved through improved acquisition techniques. These would allow more reliable capture of the iris region when the eye is fully open, minimizing specular reflections and keeping the eye region in sharp focus and high contrast. Enhanced face and eye tracking can help, in particular with the focus requirements. Note that, at 15 cm the focus depth is quite shallow and the iris region can easily lose focus to higher contrast regions of the face.

Nevertheless this study has shown that iris acquisition is practical in such a system and refined system design could greatly improve the reliability of the acquisition process leading to more acceptable levels of iris recognition performance. In conclusion, it is clear that the preliminary experiments presented here have been limited by the current optical design which is not optimized for optical differences between visible and IR wavelengths. An improved design would allow more number or a greater density of NIR pixels, thus improving the quality of the acquired images. Design strategies such as sampling colour at a very sparse set of locations and then propagating throughout the image with guidance from an unaliased monochrome NIR channel [7] could possibly be adapted for this purpose. Such a design should accommodate the required optical resolution at both NIR and visible wavelengths and achieve a large iris pixel density , with 100+ pixels across iris diameter. Realizing these design goals may require a 6 or even 8 Megapixel sensor coupled with an advanced optical design, but the front cameras on today's smartphones are already in this size ballpark.

The minimum iris size requirement for good results places a limitation on the distance to subject. Ideally it would also be possible to increase the acquisition distance from 15-20 cm to a more comfortable 25-40 cm. However this suggests an additional doubling of the sensor size to $13-16$ Megapixels, which comes with increased cost. The possibility to design, realize and test such a hybrid solution is currently being investigated.

Our conclusion is that iris biometrics can be implemented on mobile hand-held devices using hybrid visible/NIR camera modules similar to the one presented in this article. However significant challenges remain if the industry is to achieve practical working solutions that are sufficiently reliable and robust to meet the demands of today's consumers.

7. Acknowledgment

This research is funded by the employment based PhD program of the Irish Research Council (www.research.ie). Authors would like to thank Professor Christopher Dainty, Dr.Istvan Andorko and Alexandru Drimbarean for their valuable assistance in this work.

References

[1] D. Ackerman. Spatial Resolution as an Iris Quality Metric. Presented at Biometrics Consortium Conference Tampa, Florida September 28, 2011. 3, 4

[2] E. Allen and S. Triantaphillidou. *The manual of photography*. Taylor & Francis, 2011. 3, 4

[3] S. Barra, A. Casanova, F. Narducci, and S. Ricciardi. Ubiquitous iris recognition by means of mobile devices. *Pattern Recognition Letters*, (0):–, 2014. 2

[4] B. E. Bayer. Color imaging array, 1975. US Patent 3,971,065. 2

[5] K. W. Bowyer, K. Hollingsworth, and P. J. Flynn. Image understanding for iris biometrics: A survey. *Computer Vision and Image Understanding*, 110:281–307, 2008. 1

[6] C. Boyce, A. Ross, M. Monaco, L. Hornak, and X. Li. Multispectral iris analysis: A preliminary study51. In *Computer Vision and Pattern Recognition Workshop, 2006.*, pages 51–51, June 2006. 2

[7] A. Chakrabarti, W. Freeman, and T. Zickler. Rethinking color cameras. In *IEEE International Conference on Computational Photography*, pages 1–8, May 2014. 7

[8] P. Corcoran. Biometrics and Consumer Electronics: A Brave New World or the Road to Dystopia? *IEEE Consumer Electronics Magazine*, 2(2):22–33, Apr. 2013. 1

[9] P. Corcoran, P. Bigioi, and S. Thavalengal. Feasibility and design considerations for an iris acquisition system for smartphones. In *IEEE Fourth International Conference on Consumer Electronics-Berlin*, pages 164–167, Sept 2014. 2, 3, 4

[10] S. Curtis. Quarter of the world will be using smartphones in 2016. *The Telegraph*, 11 December 2014. 1

[11] J. Daugman. How Iris Recognition Works. *IEEE Transactions on Circuits and Systems for Video Technology*, 14(1):21–30, Jan. 2004. 1, 2, 3

[12] N. A. Dodgson. Variation and extrema of human interpupillary distance. In *Proc. SPIE 5291*, pages 36–46, 2004. 3

[13] D. ho Cho, K. R. Park, D. W. Rhee, Y. Kim, and J. Yang. Pupil and iris localization for iris recognition in mobile phones. In *Seventh ACIS International Conference on Software Engineering, Artificial Intelligence, Networking, and Parallel/Distributed Computing*, pages 197–201, June 2006. 2

[14] D. Jeong, H.-A. Park, K. Park, and J. Kim. Iris recognition in mobile phone based on adaptive gabor filter. In D. Zhang and A. Jain, editors, *Advances in Biometrics*, volume 3832 of *Lecture Notes in Computer Science*, pages 457–463. Springer Berlin Heidelberg, 2005. 2

[15] R. R. Jillela and A. Ross. Segmenting iris images in the visible spectrum with applications in mobile biometrics. *Pattern Recognition Letters*, (0):–, 2014. 2

[16] N. Koren. The imatest program: comparing cameras with different amounts of sharpening. volume 6069, pages 60690L–60690L–9, 2006. 4

[17] A. Kumar and A. Passi. Comparison and combination of iris matchers for reliable personal authentication. *Pattern Recognition*, 43(3):1016 – 1026, 2010. 6

[18] Y. Lu, M. Higgins-Luthman, W. Livengood, and J. Harris. Combined rgb and ir imaging sensor, 2013. US Patent 8,446,470. 2

[19] Multimedia University. MMU iris database. 6

[20] J. Nakamura. Modern Image Sensors. In T. V.Galstian, editor, *Smart Mini-Cameras*, pages 49–82. CRC Press, 2014. 4

[21] Neurotechnology. NeuroTechnology VeriEye SDK, 2015. 6

[22] OmniVision. OmniVision's OV4682. 2

[23] S. Orandi and R. M. Mccabe. Mobile ID Device Best Practice Recommendation. *Information Access Division Information Technology Laboratory NIST*, (August), 2009. 2, 3

[24] K. Park, H.-A. Park, B. Kang, E. Lee, and D. Jeong. A study on iris localization and recognition on mobile phones. *EURASIP Journal on Advances in Signal Processing*, 2008(1):281943, 2008. 2

[25] K. B. Raja, R. Raghavendra, V. K. Vemuri, and C. Busch. Smartphone based visible iris recognition using deep sparse filtering. *Pattern Recognition Letters*, (0):–, 2014. 2

[26] W. J. Smith. *Modern Optical Engineering - Third Edition*. McGraw-Hill, 2000. 3

[27] G. Sutra, B. D. e. S. Garcia-salicetti, and N. Othman. A biometric reference system for iris. Technical report, 2012. 5

[28] E. Tabassi, P. Grother, and W. Salamon. IREX II-IQCE iris quality calibration and evaluation. *NIST Interagency report*, 7820. 3

[29] The Institute of Automation of the Chinese Academy of Sciences. CASIA iris database. http://biometrics.idealtest.org/. 6

[30] Working Group. ISO/IEC 19794-6 Information Technology - Biometric Data Interchnage Formats - Part 6: Iris image. *JTC1 :: SC37, international standard edition*, 2005. 2, 3, 4